

Green syntheses, characterization and Antibacterial Activity of amorphous iron oxide nanoparticles using aqueous leaf extract of castor

Munira M. Ashrif^{*1}, Mariam S. Saleh², Safe E. Rahuma³

^{1,2} Department of Chemistry, Faculty of Science, University of Zawia, Zawia, Lidya.

³ Department of Chemistry, Faculty of Education Zaltan, Sabratha University, Zaltan, Lidya.

^{*1}Correspondence Email address: m.ashrif@zu.edu.ly

Abstract:

Iron oxide nanoparticles (IONPs) have attracted considerable interest for diverse fundamental and biomedical applications. IONPs play significant roles in nanotechnology and considered to be one of the prominently used particles due to their lesser toxicity and high chemical stability. The undertaken study describes biological synthesis of Iron Oxide nanoparticles (Fe₂O₃ NPs) using leaf Castor extract along with evaluation of the antibacterial efficiency. To synthesis the Iron oxide nanoparticles, freshly extract was added to 0.1 M solution of Iron chloride hexahydrate in a 5:1 volume ratio. The synthesis of Fe₂O₃ NPs was confirmed via several characterizations. UV–Vis analysis detected a characteristic absorbance at the spectral range of 380 nm and the energy gap was (2.4 eV). The functional groups which are responsible for nanoparticle formation have been identified by Fourier transformed infrared spectroscopy (FTIR). NPs' XRD pattern doesn't have a definite crystalline peak, thus it is obvious that IONPs are amorphous compounds by nature. α -Fe₂O₃ NPs are more efficient to inhibit the growth of Staphylococcus aureus as the zone of inhibition (ZOI) ranging from 17-22 mm and the maximum ZOI was 22 mm at concentration 75 μ g/ml have been observed. It has been seen in this study that by increasing the concentration of the α -Fe₂O₃ nanoparticles, the growth inhibition has also been increased.

Keywords: Green Synthesis, Iron Oxide Nanoparticles, leaf Castor, Inhibition Zone.

التوليفات الخضراء والتوصيف والنشاط المضاد للبكتيريا لجسيمات أكسيد الحديد النانوية غير المتبلورة باستخدام مستخلص أوراق الخروع المائي.

منيرة مفتاح الشريف^{1*} مريم صالح صالح¹ صفاء الشريف ارحومة²

1 قسم الكيمياء، كلية العلوم، جامعة الزاوية، الزاوية، ليبيا.

2 قسم الكيمياء، كلية التربية زلطن، جامعة صبراتة، زلطن، ليبيا.

m.ashrif@zu.edu.ly

الملخص:

اجتذبت الجسيمات النانوية لأكسيد الحديد (IONPs) اهتماما كبيرا بالتطبيقات الأساسية والطبية الحيوية المتنوعة. تلعب (IONPs) ادوار مهمة في تكنولوجيا النانو وتعتبر واحدة من الجزيئات المستخدمة بشكل بارز بسبب سميتها الاقل وثباتها الكيميائي العالي. تصف الدراسة التي تم اجراءها التركيب البيولوجي لجسيمات اكسيد الحديد النانوية (Fe_2O_3 NPs) باستخدام مستخلص اوراق الخروع مع تقييم الكفاءة المضادة للبكتيريا. لتخليق جسيمات اكسيد الحديد النانوية، تمت إضافة المستخلص الطازج إلى محلول 0.1 مولارى من سداسي هيدرات كلوريد الحديد بنسبة حجم 5:1. تم تأكيد تخليق (Fe_2O_3 NPs) من خلال عدة خصائص. كشف تحليل الأشعة فوق البنفسجية والمرئية عن امتصاصية مميزة عند المدى الطيفي 380 نانومتر وكانت لفجوة الطاقة (2.4 فولت). تم تحديد المجاميع الوظيفية المسؤولة عن تكوين الجسيمات النانوية بواسطة التحليل الطيفي للأشعة تحت الحمراء المحول فورييه (FTIR). لا يحتوي نمط XRD الخاص بـ NPs على أي ذروة بلورية محددة، وبالتالي فمن الواضح ان IONPs عبارة عن مركبات غير متبلورة بطبيعتها. تعتبر Fe_2O_3 NPs α - أكثر كفاءة في تثبيط نمو المكورات العنقودية الذهبية حيث ان منطقة التثبيط (ZOI) تتراوح بين 17-22 ملم وقد لوحظ أن الحد الأقصى

ZOI كان 22 ملم عند التركيز 75 ميكروغرام / مل. وقد لوحظ في هذه الدراسة انه من خلال زيادة تركيز الجسيمات النانوية $\alpha\text{-Fe}_2\text{O}_3$ ، تم ايضا زيادة تثبيط النمو. الكلمات المفتاحية : التخليق الاخضر، جزيئات اكسيد الحديد النانوية، نبات الخروع، منطقة التثبيط.

Introduction:

Nanotechnology deals with the nanosized particles and involves the production and manipulation of stronger and lighter materials at the nanometer scale (Benelmekki., 2015; Chavali&Nikolova., 2019 andKhan et al., 2022). Nanotechnology is useful and bring benefits in diverse areas such as water decontamination, biology, chemistry, drug development. Nanoparticles (NPs) produced by nanotechnology are group of atoms and molecules in the range of 1 – 100 nm and can be composed of one or more species of atoms or molecules (Benelmekki.,2015). The creations of nanoparticles (NPs) are either by scaling up from single groups of atoms or by refining or reducing bulk of materials (Chavali&Nikolova., 2019). NPs can reveal an extensive range of size dependent properties.

Recently, iron oxide nanoparticles have attracted considerable interest for diverse fundamental and biomedical applications. Iron oxide nanoparticles having size and width of 10-100 nm play significant roles in nanotechnology (Nair et al., 2021) and considered to be one of the prominently used particles due to their lesser toxicity and high chemical stability (Abbaszadeh& Hejazi., 2019). Iron oxide nanoparticles ($\alpha\text{-Fe}_2\text{O}_3$, $\gamma\text{-Fe}_2\text{O}_3$, Fe_3O_4 and FeO) possess super paramagnetic properties. Hematite ($\alpha\text{-Fe}_2\text{O}_3$) nanoparticle is one of different polymorphs of iron oxide. $\alpha\text{-Fe}_2\text{O}_3$ nanoparticles are more appropriate for biomedical application because of their high chemical stability and less toxicity (Abbaszadeh& Hejazi., 2019).

Many methods have been reported for iron oxide nanoparticles synthesis, such as physical, chemical and biological methods (Khan et al., 2022 and Allafchian et al., 2019). The physical method supports the particle size in the nanometer range (Alphandéry 2019), while the chemical preparation method is very simple, and regulates

the morphology, scale, and some additional properties of nanoparticles (Amanzadeh et al., 2019). There are many physical and chemical methods for synthesis of INPs, However, chemical routes that involves usage of toxic solvents, which could possibly create dangerous byproducts, and physical methods usually require high energy and vacuum (Pallela et al., 2019). The comparison between the mentioned methods suggest that the biological process of nanoparticle synthesis is cost effective, efficient for large-scale production and ecofriendly procedure (Khan et al., 2022 and Abou El-Nour et al., 2010). In addition, there is no requirement for high pressure, energy, temperature or toxic chemicals. Plant extracts are among the most used and abundant compounds for green synthesis in nano-chemistry. The biological synthesis of Iron oxide nanoparticles using plant extracts can be mono-dispersed by controlling parameters, such as temperature, pH and mixing ratio (Benelmekki.,2015). In this method, a variety of metabolites acts as reducing agents in NPs synthesis. Recently, synthesizing metal and metal oxide nanoparticles using plants has been extensively studied. The biological nanoparticles have been found to be more pharmacologically active than physic chemically synthesis nanoparticles (Akhtar et al., 2013; Prasad et al., 2014; Ali et al., 2016; Wu et al., 2008 and Teja & Koh.,2009). Plants serve as reducing and capping agents involved in the synthesis procedure which is considered ecofriendly (Bar et al 2009 and Sangaru et al., 2003). Each part of the plant can be used for nanoparticle synthesis, such as the leaves, flowers, straws, stems (Bar et al., 2009; Sangaru et al., 2003; Armendariz et al., 2004; Armendariz et al., 2011; Herrera et al., 2003; Gardea-Torresdey et al., 2003 and Huang et al., 2007). The leaf extract acts as an environmental reducing agent that is nonhazardous and nontoxic (Kouhbananiet al., 2019). Particularly, Nanoparticles produced by medicinal plant have been found to the most pharmacologically active and this because of the attachment of several pharmacological active residues. Castor plant has been used for medicinal purposes. The Preliminary Phytochemical study of castor leaves revealed the presence of many active phytochemicals including steroids, phenolic acid, alkaloids,

flavonoids, glycosides, and polyphenols, which act as bio-reductants and stabilizing agent (Jena & Gupta2012).The study aims to biologically synthesis α -Fe₂O₃ NPs using castor plant extract as reducing agents and measure the antibacterial activity of produced α -Fe₂O₃ NPs.

2. Materials and Methods

2.1. Materials

Fresh castor plant leaves were gathered at Al-Zawia city / Libya. Iron chloride hexahydrate (FeCl₃.6H₂O) was purchased from Sigma Aldrich. The test organisms selected include both gram-positive bacteria, Staphylococcus aureus and Staphylococcus spp and gram negative bacteria, Escherichia coli, Klebsiella pneumonia.

2.2. Preparation of Leaf Extract

Green castor leaves were collected from Zawia city. The extract was made by cutting 20 g of castor leaves into small pieces, washing them in distilled water to get rid of any contaminants, and then adding them to an Erlenmeyer flask with 100 ml of distilled water. The mixture was heated on hot plate 100°C for 15 minutes, cooled, and then filtered by what man filter and funnel filter. The obtained fine solution (brown color) was collected and stored at 4°C for further use to synthesis Iron oxide nanoparticles.

2.3. Synthesis of Iron Oxide Nanoparticles

To synthesis the Iron oxide nanoparticles, freshly extract was added to 0.1 M solution of Iron chloride hexahydrate in a 5:1 volume ratio. The precursor solution 0.1 M FeCl₃.6H₂O changed color from brown to black and precipitate was formed after addition of Castor extract. The nanoparticles were separated by centrifuging at 15000 rpm for 10 min. The obtained precipitates were washed by ultrapure water and dried in the open air for 24 hours, and then subjected to characterization. The process to synthesis of Fe₂O₃ NPs with plants is shown in figure 1 (Dhananjayan et al., 2017 and Shtewiet al., 2021).

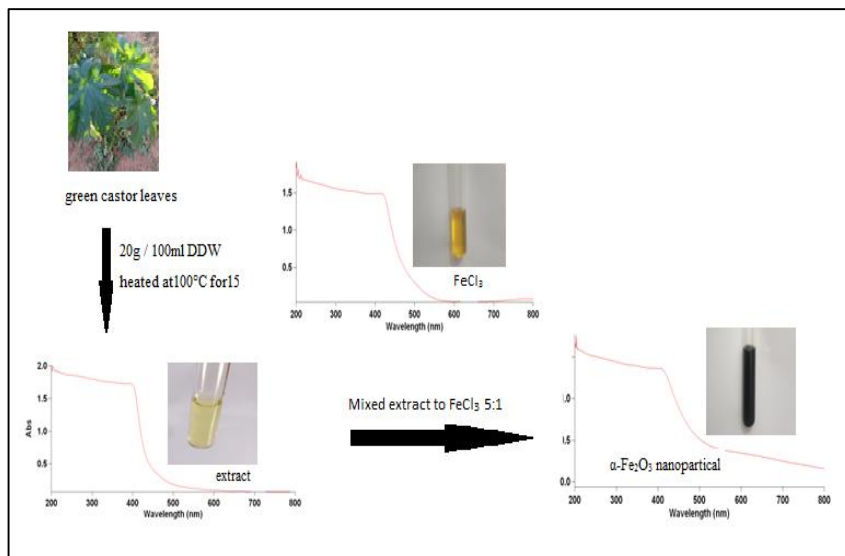


Figure 1. The process of a UV-visible spectrophotometer used to characterize α -Fe₂O₃ nanoparticles.

2.4. Characterization of iron oxide nanoparticles

Using the Shimadzu XRD-6100 diffract meter, the sample's crystal structure was examined and Copper K α radiation ($\lambda=1.54060 \text{ \AA}$) was used to capture the patterns. Using an IR Affinity-1S (Shimadzu) spectrometer, Fourier transform infrared (FT-IR) spectroscopy was used for the identification of major chemical groups present with Fe₂O₃ NPs. The spectrometer recorded wavenumbers between 450 and 4,000 cm⁻¹. Via UV-Vis-NIR Spectroscopy (5000), the sample's maximal optical absorption in the 200–800 nm range was determined. α -Fe₂O₃ nanoparticles' optical properties were examined by measurement using an ultraviolet-visible (UV-vis) spectrophotometer.

3. Results and discussions

3.1. FT-IR Spectroscopy:

The binding of iron to phytochemical compounds included in the aqueous extract of castor plant leaves (Suurbaar et al., 2017 and Altameme et al., 2015) was investigated using FT-IR measurements. The FT-IR spectrum of the synthesized Fe₂O₃ nanoparticles, which

shows the functional groups and chemical bonds of the compound, ranged from 400 to 4000 cm^{-1} in figure 2. The stretching vibrations in the OH groups are responsible for the enormous broad band that appears at 3409 cm^{-1} . The weak peak at 2977 cm^{-1} is attributed to asymmetric and symmetric C-H stretching mode of aliphatic hydrocarbon (Razack et al., 2020). The asymmetric and symmetric bending vibration of C = O is responsible for the absorption picks at 1645 cm^{-1} and 1388 cm^{-1} . Fe-O stretching mode is ascribed to the strong band below 879 cm^{-1} . From 550 - 603 cm^{-1} , the band associated with the Fe-O stretching mode of Fe_2O_3 can be seen (Jamzad & Kamari Bidkorpeh., 2020).

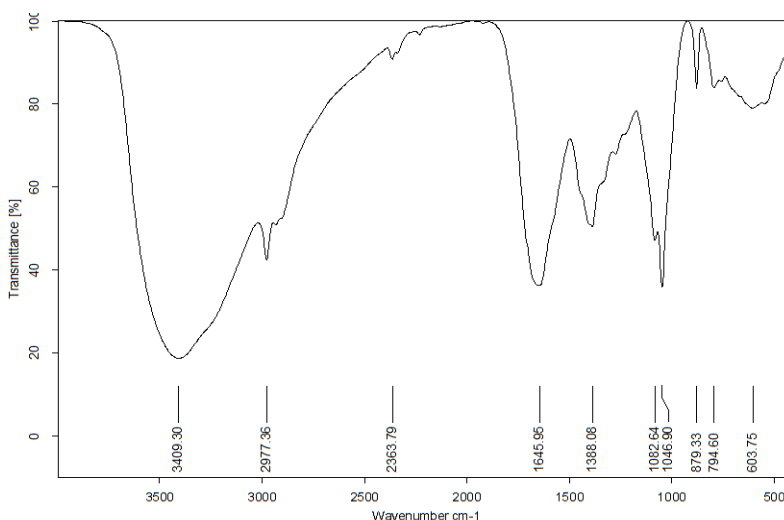


Figure 2. FT-IR Spectra of $\alpha\text{-Fe}_2\text{O}_3$ nanoparticles

3.2. X-ray Diffraction (XRD):

Figure 3 displays the $\alpha\text{-Fe}_2\text{O}_3$ NPs' XRD pattern. Since it doesn't have a definite crystalline peak, it is obvious that IONPs are amorphous compounds by nature (Yadav et al., 2020; Ajinkya et al., 2020 and Yadav et al., 2022). They had previously been able to create amorphous $\alpha\text{-Fe}_2\text{O}_3$ NPs using pomegranate peel extract (Yadav et al., 2022). It was proposed that the organic components in the leaf extract, which stabilize and coat the nanoparticles, were responsible for the broad weak peak of (2θ) between 10° and 30°

Hassan et al., 2018). Consequently, the size (2 theta) of the nanoparticles was difficult to ascertain by the detection of diffraction peaks, and this was completely consistent with the previously mentioned FTIR for the presence of the Fe-O beam. Furthermore, it has been noted that amorphous α -Fe₂O₃NPs work better than metallic iron nanoparticles or nano-or polymorphic crystals same diameter (Machala et al., 2007).

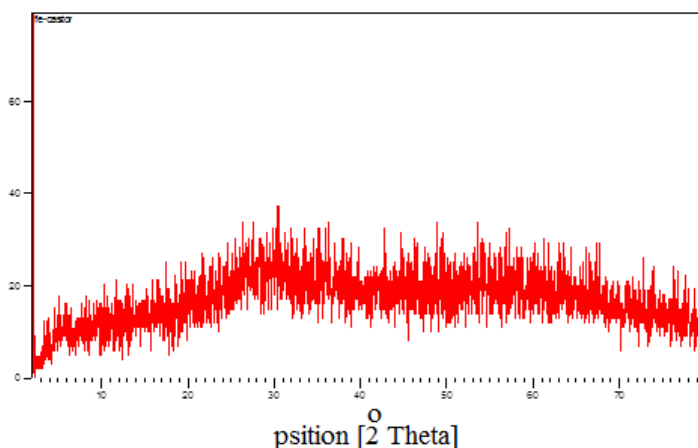


Figure 3. XRD pattern of α -Fe₂O₃ nanoparticles

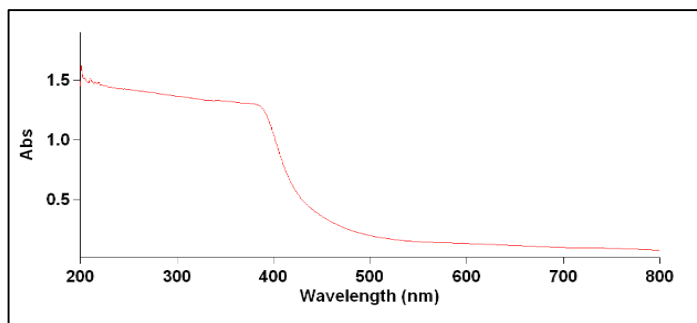
3.3. UV-Vis spectroscopy

The reduction of iron chloride in the presence of aqueous castor plant extract was generally observed by the color change of the reaction mixture, which indicated the formation of nanoparticles. Next, UV-Vis spectroscopy was used to characterize the green synthesized iron oxide nanoparticles. It was taken once the nanoparticles were formed. The absorbance spectrum was recorded in the range of 200 nm to 800 nm. Figure 4 reveals the UV-vis absorption spectrum and Tauc plot of the synthesized α -Fe₂O₃ nanoparticles. Figure (4 a) shows the maximum absorption peak at 380 nm, suggesting the synthesis of Fe₂O₃ NPs. This result is consistent with previous report, which indicated that the highest Fe₂O₃-NPs adsorption value was 380 nm (Shejawal et al., 2020 and Hammad et al., 2022). α -Fe₂O₃ is an n-type semiconductor with a

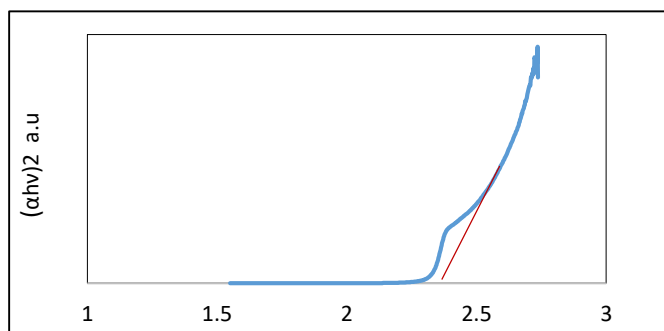
narrowband gap. The band gap energy calculated here for the synthesized nanoparticles figure (4 b) was found to be 2.4 eV, which is in a good agreement with reported value (2.5 eV) (Urabe & Aziz., 2019). The value of energy gap (2.4eV) is as a result of small size molecules and quantum confinement (Shejawal et al., 2020; Hammad et al., 2022 and Urabe & Aziz., 2019). The optical band gap (E_g) value was computed from the Tauc plot using the following equation:

$$\alpha = \frac{A (h\nu - E_g)^n}{h\nu} \quad (1)$$

Where: α is the absorption coefficient, E_g is the optical band gap of α -Fe₂O₃ nanoparticles, A is a constant, $h\nu$ is the energy of the photon, n is the nature of transitions.



(a)



(b)

Figure 4. (a) UV-Vis spectrum and (b) Ban gap energy of α -Fe₂O₃ NPs

A UV-Vis spectrophotometer was employed to assess the iron oxide nanoparticles' stability. The absorption peak occurred at a wavelength of 383 nm, and the first absorption band was seen right after synthesis. After then, it was monitored for 15 days, as shown by the absorption bands in figure 5. The graph indicates that iron oxide nanoparticles exhibit absorption values at the same peak wavelength (383 nm) throughout a period of 15 days. Regarding the variation in absorbency intensity resulting from the sample's dilution before to measurement. The steady state of the nanoparticles is shown by wavelength constancy.

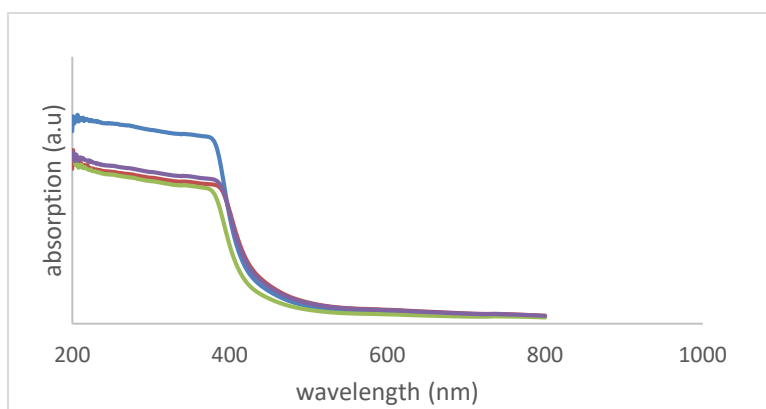


Figure 5. UV-Vis spectrum of α -Fe₂O₃ NPs over 15 days

3.4. Antibacterial activity of the biosynthesized

The α -Fe₂O₃ nanoparticles are more appropriate for biomedical application because of their high chemical stability and less toxicity (Pallela et al., 2019). Therefore, antibacterial activity of green synthesized α -Fe₂O₃ nanoparticles at different concentrations (25 μ g/ml, 50 μ g/ml, 75 μ g/ml) have been examined and significant zone of inhibitions (ZOI). In the present study, we have tested the antibacterial activity of α -Fe₂O₃ NPs which was performed against *Escherichia coli*, *Klebsiella pneumonia*, *Staphylococcus aureus* and *Streptococcus spp* using the agar well-diffusion method. ZOI showed in figure 6 were measured in millimeter, and the data were recorded. From the values of zone of inhibitions in Table 1, α -Fe₂O₃ NPs are more efficient to inhibit the growth of *Staphylococcus*

aureus as the zone of inhibition (ZOI) ranging from 17-22 mm and the maximum ZOI was 22 mm at concentration 75 $\mu\text{g/ml}$ have been observed.

It has been seen in this study that by increasing the concentration of the $\alpha\text{-Fe}_2\text{O}_3$ nanoparticles, the growth inhibition has also been increased. The size of inhibition zone was different according to the type of bacteria and the concentrations of $\alpha\text{-Fe}_2\text{O}_3$ nanoparticles.

Table 1: Zone of Inhibition (ZOI) of $\alpha\text{-Fe}_2\text{O}_3$ NPs against for types of Bacteria at different concentrations

Bacterium Types	Sample Code	ZOI (mm) of $\alpha\text{-Fe}_2\text{O}_3$ NPs at different concentrations		
		25 $\mu\text{g/ml}$	50 $\mu\text{g/ml}$	75 $\mu\text{g/ml}$
Escherichia coli	A	10	11	12
Klebsiella pneumonia	B	0	10	11
Streptococcus spp	C	0	10	12
Staphylococcus aureus	D	17	19	22

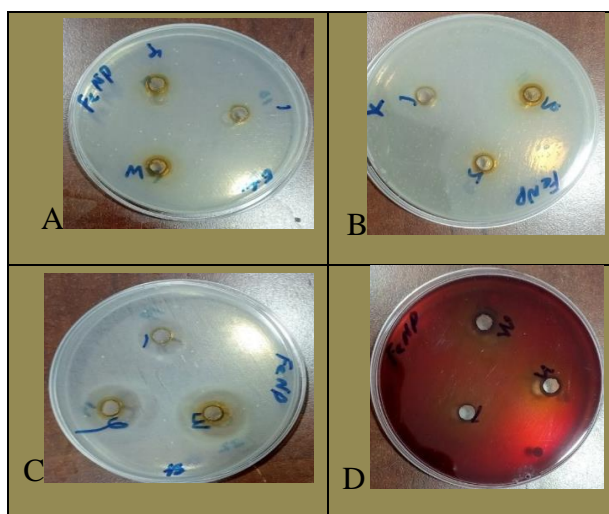


Figure 6. Bacterial cultures showing the inhibition zones around wells loaded with 25, 50, 75 $\mu\text{g/ml}$ of $\alpha\text{-Fe}_2\text{O}_3$ NPs and (A) Escherichia coli, (B) Klebsiella pneumonia, (C) Streptococcus spp, (D) Staphylococcus aureus.

4. Conclusion:

Ecologically benign and simple biosynthesis of iron oxide nanoparticles was carried out in the current investigation. Green castor leaf extract is used in its production as a covering and reducing agent. Under ideal circumstances, the generated α -Fe₂O₃-NPs were characterized. Our research showed that the castor plant significantly produces iron oxide nanoparticles through biosynthesis. Special bands for OH groups, carbonyl groups, and other groups compounds that constitute the α -Fe₂O₃-NPs were detected using FTIR, along with the FeO bands that are exclusive to α -Fe₂O₃-NPs. The UV spectra revealed that the energy band gap was 2.5 and the absorption band had a wavelength of 383 nm. It was feasible to verify that nanoparticles had formed. It is evident from the NPs' lack of a distinct crystalline peak in their XRD pattern that IONPs are amorphous compounds by nature. The end findings showed that even after 15 days, α -Fe₂O₃ NPs exhibited good stability. the appearance of an inhibitory zone demonstrates the antibacterial activity of α -Fe₂O₃ nanoparticles, since the effect rises with increasing concentration of α -Fe₂O₃-NPs. Staphylococcus aureus was more susceptible than other species.

Acknowledgements:

Authors are grateful to the Department of Chemistry Zawia University, The National Center for Medical Research at Zawia and Libyan Petroleum Institute in Tripoli for approving and facilitating this study.

References:

- Abbaszadeh, M & Hejazi, P. (2019). Metal affinity immobilization of cellulase on Fe₃O₄ nanoparticles with copper as ligand for biocatalytic applications. Food Chemistry. 290. 47-55. 10.1016/j.foodchem.2019.03.117.
- Abou El-Nour, K. M., Eftaiha, A. A., Al-Warthan, A., and Ammar, R. A. (2010). Synthesis and applications of silver nanoparticles. Arab. J. Chem. 3, 135–140. doi: 10.1016/j.arabjc.2010.04.008
- Ajinkya, N., Yu, X., Kaithal, P., Luo, H., Somani, P. and Ramakrishna, S. (2020). Magnetic Iron Oxide Nanoparticle

- (IONP) Synthesis to Applications: Present and Future. Materials (Basel, Switzerland), 13(20), 4644. <https://doi.org/10.3390/ma13204644>
- Akhtar, M. S. & Panwar, J & Yun, Y. S. (2013). Biogenic synthesis of metallic nanoparticles by plant extracts. ACS Sustainable Chemistry & Engineering. 1. 591-602.
- Ali A, Zafar H, Zia M, ul Haq I, Phull AR, Ali JS, Hussain A. (2016). Synthesis, characterization, applications, and challenges of iron oxide nanoparticles. Nanotechnol Sci Appl.94, PP 9-67 <https://doi.org/10.2147/NSA.S99986>
- Allafchian, A., Mousavi, Z. S. and Hosseini, S. S. (2019). Application of cress seed musilage magnetic nanocomposites for removal of methylene blue dye from water. Int. J. Biol. Macromol 136, pp 199–208. doi: 10.1016/j.ijbiomac.2019.06.083
- Alphandéry E. (2019). Biodistribution and targeting properties of iron oxide nanoparticles for treatments of cancer and iron anemia disease. Nanotoxicology, 13(5), 573–596. <https://doi.org/10.1080/17435390.2019.1572809>
- Altameme, H & Hussein, A & Hameed, I & Kareem, M. (2015). Determination of alkaloid compounds of Ricinus communis by using gas chromatography- mass spectroscopy (GC-MS). Journal of medicinal plant research. 9. 349-359. 10.5897/JMPR2015.5750.
- Amanzadeh, E., Esmaeili, A., Abadi, R. E. N., Kazemipour, N., Pahlevanneshan, Z. and Beheshti, S. (2019). Quercetin conjugated with superparamagnetic iron oxide nanoparticles improves learning and memory better than free quercetin via interacting with proteins involved in LTP. Sci. Rep. 9, 1–19. doi: 10.1038 s41598-019-43345-w
- Armendariz, V., Gardea-Torresdey, J., Yacaman, M., Gonzalez, J., Herrera, I. and Parsons, J. (2011). Gold nanoparticle formation by oat and wheat biomasses.
- Armendariz, V., Herrera, I., peralta-vidua, J., Yacaman, M., Troiani, H., Santiago, P. and Gardea-Torresdey, J. (2004). Size controlled gold nanoparticle formation by Avena sativa

- biomass: Use of plants in nanobiotechnology. *Journal of Nanoparticle Research*. 6. 377-382. 10.1007/s11051-004-0741-4.
- Bar, H., Bhui, D. K., Sahoo, G. P., Sarkar, P., De, S.P, Misra, A. (2009). Green synthesis of silver nanoparticles using latex of *Jatropha curcas*. *Colloids and Surfaces A: Physicochemical and Engineering Aspects*, 339, pp. 134–139.
- Benelmekki, M. (2015). An introduction to nanoparticles and nanotechnology.
- Chavali, M.S., Nikolova, M.P. (2019). Metal oxide nanoparticles and their applications in nanotechnology. *SN Appl. Sci.* 1, 607. <https://doi.org/10.1007/s42452-019-0592-3>
- Dhananjayan, B., Thirumalai, D. and Asharani, Indira. (2017). Green Synthesis of Iron Oxide Nanoparticles Mediated by *Actinodaphne madraspatna* Bedd Leaves. *Asian Journal of Chemistry*. 29. 2446-2448. 10.14233/ajchem.2017.20758.
- Gardea-Torresdey, J., Gomez, E., peralta-vidua, J., Parsons, J., Troiani, H. and Yacaman, M. (2003). Alfalfa Sprouts: A Natural Source for the Synthesis of Silver Nanoparticles. *Langmuir*. 19. 10.1021/la020835i.
- Hammad, E. N., Salem, S. S., Mohamed, A. A., & El-DougDoug, W. (2022). Environmental Impacts of Ecofriendly Iron Oxide Nanoparticles on Dyes Removal and Antibacterial Activity. *Applied biochemistry and biotechnology*, 194(12), 6053–6067. <https://doi.org/10.1007/s12010-022-04105-1>
- Hassan, S & Abdel-Shafy, H & Mansour, M. (2018). Removal of pyrene and benzo(a)pyrene micropollutant from water via adsorption by green synthesized iron oxide nanoparticles. *Advances in Natural Sciences: Nanoscience and Nanotechnology*. 9. 015006. 10.1088/2043-6254/aaa6f0.
- Herrera, I., Gardea-Torresdey, J., Tiemann, K.J., peralta-vidua, J., Armendariz, V., and Parsons, J. (2003). Binding of Silver(I) Ions by Alfalfa Biomass (*Medicago Sativa*): Batch PH, Time, Temperature, and Ionic Strength Studies. *J. Hazard. Subst. Res.* 4. 1-16. 10.4148/1090-7025.1026.

- Huang, J., Li, Q., Sun, D., Lu, Y., Su, Y., Yang, X., Wang, H., Wang, Y., Shao, W., He, N., Hong, J. and Chen, C. (2007). Biosynthesis of silver and gold nanoparticles by novel sundried Cinnamomum camphora leaf. *Nanotechnology*. 18. 105104. 10.1088/0957-4484/18/10/105104.
- Jamzad, M., & Kamari Bidkorpheh, M. (2020). Green synthesis of iron oxide nanoparticles by the aqueous extract of *Laurus nobilis* L. leaves and evaluation of the antimicrobial activity. *Journal of Nanostructure in Chemistry*, 10, 193 - 201. <https://doi.org/10.1007/s40097-020-00341-1>
- Jena, J. and Gupta, A. (2012). *Ricinus communis* linn: A phytopharmacological review. *International Journal of Pharmacy and Pharmaceutical Sciences*. 4. 25-29.
- Khan, S., Bibi, G., Dilbar, S., Iqbal, A., Ahmad, M., Ali, A., Ullah, Z., Jaremko, M., Iqbal, J., Ali, M., Haq, I. and Ali, I. (2022). Biosynthesis and characterization of iron oxide nanoparticles from *Mentha spicata* and screening its combating potential against *Phytophthora infestans*. *Frontiers in plant science*, 13, 1001499. <https://doi.org/10.3389/fpls.2022.1001499>
- Kouhbanani, M., Beheshtkhoo, N., Taghizadeh, S., Amani, A. and Alimardani, V. (2019). One-step green synthesis and characterization of iron oxide nanoparticles using aqueous leaf extract of *Teucrium polium* and their catalytic application in dye degradation. *Advances in Natural Sciences: Nanoscience and Nanotechnology*. 10. 015007. 10.1088/2043-6254/aafe74.
- Machala, L. Zboril, R. and Gedanken, A., (2007). Amorphous Iron(III) Oxide A Review. *Phys. Chem . B* 111 4003.
- Nair, G & T Thannickal, S & Mathew, B. (2021). Advanced Green Approaches for Metal and Metal Oxide Nanoparticles Synthesis and Their Environmental Applications. *Talanta Open*. 5. 100080. 10.1016/j.talo.2021.100080.
- Pallela, P & Shameem, U. & Ruddaraju, L. & Gadi, S. & Cherukuri, C. & Barla, S. & Pammi, S.V.N. (2019). Antibacterial efficacy of green synthesized α -Fe₂O₃ nanoparticles using *Sida cordifolia* plant extract. *Heliyon*. 5. e02765. 10.1016/j.heliyon.2019.e02765.

- Prasad, K. S. & Gandhi, P. & Selvaraj, K. (2014). Synthesis of green nano iron particles (GnIP) and their application in adsorptive removal of As(III) and As(V) from aqueous solution. *Applied Surface Science*. 317. 1052-1059. 10.1016/j.apsusc.2014.09.042.
- Razack, S & Suresh, A & Sriram, S & Ramakrishnan, G & Sadanandham, S & Veerasamy, M & Nagalamadaka, R & Sahadevan, R. (2020). Green synthesis of iron oxide nanoparticles using Hibiscus rosa-sinensis for fortifying wheat biscuits. *SN Applied Sciences*. 2. 10.1007/s42452-020-2477-x.
- Sangaru, S. S., Ahmad, A., Pasricha, R., Sastry, M. (2003). Bioreduction of chloroaurate ions by Geranium leaves and its endophytic fungus yields gold nanoparticles of different shapes. *Journal of Materials Chemistry*. 13. 1822-1826. 10.1039/B303808B.
- Shejawal, K. P., Randive, D. S., Bhinge, S. D., Bhutkar, M. A., Wadkar, G. H., & Jadhav, N. R. (2020). Green synthesis of silver and iron nanoparticles of isolated proanthocyanidin: its characterization, antioxidant, antimicrobial, and cytotoxic activities against COLO320DM and HT29. *Journal, genetic engineering & biotechnology*, 18(1), PP 1-11. <https://doi.org/10.1186/s43141-020-00058-2>
- Shtewi, F. A., Barag, W. M., Tarroush, A. A. (2021). Green Synthesis and Characterization of Iron Oxide Nanoparticles Using MenthaPiperita Leaves Extract. *International Science and Technology Journal*. 24. DOI: 10.13140/RG.2.2.16073.36965.
- Suurbaar, J & Mosobil, R & Donkor, A. M . (2017). Antibacterial and antifungal activities and phytochemical profile of leaf extract from different extractants of Ricinus communis against selected pathogens. *BMC Research Notes*. 10. 660. 10.1186/s13104-017-3001-2.
- Teja, A & Koh, P. Y. (2009). Synthesis, properties, and applications of magnetic iron oxide nanoparticles. *Prog. Cryst. Growth Charact. Mater.*. 55. 22-45. 10.1016/j.pcrysgrow.2008.08.003.

- Urabe. A. A and Aziz. W. J. (2019). Assessment of Antimicrobial Activity of Phytofabricated Iron Oxide Nanoparticles. *Plant Archives*. 19(1), pp. 600-604.
- Wu, W., He, Q., & Jiang, C. (2008). Magnetic iron oxide nanoparticles: synthesis and surface functionalization strategies. *Nanoscale research letters*, 3(11), 397–415. <https://doi.org/10.1007/s11671-008-9174-9>
- Yadav, V. K, Daoud A, Samreen H. K, Govindhan G, Nisha C and et al. (2020). "Synthesis and Characterization of Amorphous Iron Oxide Nanoparticles by the Sonochemical Method and Their Application for the Remediation of Heavy Metals from Wastewater" *Nanomaterials* 10, no. 8: 1551. <https://doi.org/10.3390/nano10081551>
- Yadav, V. K., Gnanamoorthy, G. Ali, D., Bera, S.P., Roy, A., Kumar, G., Choudhary, N., Kalasariya, H., Basnet, A. and Velmurugan, P. (2022). Cytotoxicity, Removal of Congo Red Dye in Aqueous Solution Using Synthesized Amorphous Iron Oxide Nanoparticles from Incense Sticks Ash Waste. *J. Nanomaterials*. <https://doi.org/10.1155/2022/5949595>